J Mater Sci (2006) 41:7537–7544
DOI 10.1007/s10853-006-0838-5

Fatigue property of semisolid A357 aluminum alloy under different heat treatment conditions

Yong X. Gan · Ruel A. Overfelt

Received: 30 September 2005 / Accepted: 23 November 2005 / Published online: 19 September 2006

Abstract Effect of heat treatment conditions on fatigue property of a semisolid A357 aluminum alloy under cyclic tensile loading was investigated. Comparison of the fatigue property of the semisolid A357 under T5 and T6 heat treatment conditions with other aluminum alloys including conventional casting A357-T6 alloy and four wrought aluminum alloys: 2024-T4, 7075-T6, 5052-T6 and 6061-T6 was made. It is found that the fatigue strength of the semisolid A357 under both heat treatment conditions is much higher than that of the casting A357-T6 alloy, comparable to that of the 6061-T6, but lower than that of the 2024-T4 and 7075-T6. Two-parameter Weibull distribution of fatigue data for the semisolid A357 under the two heat treatment conditions was constructed to show the statistical significance in fatigue lifetime. Fatigue fracture surface of the semisolid A357 under T5 and T6 heat treatment conditions was examined using scanning electron microscope (SEM). In the stable crack propagation region, the semisolid A357-T5 shows fatigue damage species of severely deformed grains, void coalescence, striations and ridgelines, while the A357-T6 displays less plastic deformation as revealed by the fatigue damage features of intergranular cracks, and transgranular cleavage patterns.

Y. X. Gan (✉)
Department of Mechanical Engineering, Albert Nerken School of Engineering, The Cooper Union for the Advancement of Science and Art, 51 Astor Place, New York City, NY 10003, USA
e-mail: gan@cooper.edu

R. A. Overfelt
Materials Engineering Program, Department of Mechanical Engineering, Auburn University, 201 Ross Hall, Auburn, AL 36849-5341, USA

Introduction

Semisolid processes have several advantages over conventional casting processes. First, semisolid materials have very dense microstructures because semisolid processes involve both casting and compressive deformation at elevated temperatures [1–3]. Thus, casting defects such as gaseous pores, shrinkage cracks can be effectively eliminated. Second, segregations and dendrites as often found in conventional casting processes can be reduced into minimum extent in semisolid processes [4]. Alloys during semisolid processes are in liquid and solid mixed state and are filled into the space of dies in laminar flow. Since solidification times are considerably short and cooling rates are homogeneous in the alloys, segregations have little chance to occur [5]. The growth of dendrites is also inhibited or even totally prevented. Such features of semisolid forming processes provide materials with very good mechanical properties. By precise design of dies, semisolid-formed parts are in net-shape with excellent dimension accuracy so that post machining, salvaging and scrapping of the parts are not necessary [6], which can save materials and can cut manufacturing costs.

Semisolid forming processes have been studied in several aspects including microstructure dependence on processing parameters. In the work performed by

Witulski et al. [7], microstructures of rapidly-compressed slugs were investigated. A form factor (*FF*) was proposed for estimation of spheroidicity of the structures. The expression for the form factor is $FF = 4\pi A/P^2$, where A is the area and P the perimeter of the structures. By definition, a form factor of 1 corresponds to a perfect sphere. Typically, an *FF* over 0.6 is desirable for industrial applications. Kapronos, Liu, Atkinson and Kirkwwod [8] studied the effect of temperature and soaking time on the form factor of an A356 alloy. The process parameters were optimized and a model for characterizing the flow of the semisolid alloy slurry was proposed. Jung and Kang [9] reported their work on an optimal coil design to reduce temperature gradient of billets and to obtain globular microstructures. Induction heating experiments were performed on A356 alloys to validate the theoretically proposed processing parameters such as reheating time, holding temperature, holding time, adiabatic material dimension and capacity of the induction heating system. It was found that holding time is the most critical factor for obtaining fine globular microstructures.

Semisolid forming die design is another aspect that is extensively studied. Since semisolid materials have to travel a relatively long distance to fill the cavity of dies, effect of gate shapes of dies on the formation of defects in semisolid parts has been investigated. Die design by computer simulation based on fluid-solidification analysis of an A357 alloy was studied [10]. Metal filling phenomena associated with die design were also performed and correlated with the processing parameters. A newly designed gating system considering thermal fluid properties and solidification phenomena was proposed based on the computer simulation of three dimensional metallurgical filling. Barkhudarov et al. investigated the three-dimensional thixotropic flow [11]. A model and sets of modified programs were proposed for analysis of the thixotropic behavior at different fraction of solid (f_s), shear rate and compressive velocities. Such results are useful in analysis of rapid compression on semi-solid slugs of A357 aluminum alloys [12], which may assist die design in commercialization of semisolid forming processes.

Evaluation of mechanical properties of semisolid materials is also an important topic because it can provide very useful information about the structure–property relationship of the materials and assist in optimizing processing parameters. High temperature deformation behavior of semisolid aluminum alloys including A357 under various compressive loading conditions was studied [4]. The compressive tests were conducted in the temperature range from 565 °C to 585 °C at various compressive speeds from 1 mm/s to 1000 mm/s. Test results at even higher compressive speeds, up to 2000 mm/s, were also given [10]. It was found that in the strain range from 0 to 10%, the stress of the semisolid A357 alloy increased monotonically. In the strain range higher than 10%, plastic flow behavior was observed; the stress deceased for strain rate higher than 29.4 s^{-1}. The stress–strain curves were used for optimizing processing parameters such as pressure, ram velocity and temperature for preventing liquid segregation.

Room temperature mechanical properties of semisolid aluminum alloys with various alloying elements, microstructures, and under different heat treatment conditions were studied [3]. Mechanical property data were obtained by tensile tests on specimens from various locations of the parts. The effect of alloy composition and heat treatment condition on the mechanical properties was also evaluated. It was found that the elongation of the semisolid A357 is comparable to that of the hot extruded 2024 with an extrusion ratio of 9.37, while the ultimate tensile strength of the semisolid A357 is about 10% lower than that of the extruded 2024. It was also found that the ultimate tensile strength and elongation data were more scattered for circular bar and sheet specimens of the two alloys without heat treatment. After heat-treated under T6 condition, the semisolid A357 bar and sheet specimens displayed much more uniform elongation. In addition, the ultimate tensile strength of the semisolid A357 increased more than that of the wrought aluminum alloy and the ultimate tensile strength of the sheet specimens for the semisolid A357 is slightly (about 7%) higher than that of the sheet specimens of the wrought 2024 alloy.

Fatigue properties of conventional casting aluminum alloys are very sensitive to casting defects and in most cases both crack initiation lifetime and crack propagation lifetime are controlled by defects [13–15]. Since it is very difficult to remove the intrinsic metallurgical defects in the conventional castings completely, improvement of fatigue property depends mainly on modification of the composition and microstructural constituents of casting aluminum alloys [16, 17]. High cycle fatigue behavior of cast aluminum alloys, for example A357 alloy, has been performed to obtain *S–N* curves for application design. Typical data is shown in [18]. Thermal–mechanical fatigue properties of casting aluminum alloys have been studied for specific applications in automobile industry [19]. Strain controlled fatigue tests were performed on Al–Si–Mg casting alloys with similar composition to A356/357 alloys. Cyclic hardening behavior of such alloys for

application as cylinder head materials in car engines was found in the temperature range from 200 °C to 400 °C. Comparative studies of thermal–mechanical fatigue properties on a reinforced alloy containing 15% discontinuous alumina fiber and that of without the fiber reinforcement were made.

Heat treatment is considered as an important factor that affects the fatigue behavior of casting aluminum alloys. Caton et al. [20] reported their work on the behavior of small fatigue cracks. Solution treatment followed by both peak-ageing (T6) and over-peak ageing conditions (T7) was performed on the cast aluminum alloy with a composition of Al–7.43Si–3.33Cu–0.24Mg. Small crack growth data showed that the fatigue crack speed for the specimens under the peak aged heat treatment condition (T6) is lower than that for the specimens under over peak aged heat treatment (T7).

Bergsma et al. [21] studied the fatigue behavior of a semisolid A357-T6 alloy. Fatigue tests were performed at 1 Hz with a minimum to maximum stress ratio $R = -1$. It is found that the fatigue property of the semisolid A357-T6 is superior to conventional casting A357 alloys. Heat treatment of the semisolid alloy is considered as one of the dominant factors that control the fatigue properties of the material. For components made of semisolid A357 alloys, post heat treatments such as T5 and T6 have applied for further improving the performance of the semisolid parts under service conditions. Earlier studies have proven that the ultimate tensile strength of semisolid formed parts under T6 heat treatment condition is the highest among various heat treatment conditions [3, 20]. The fine precipitates of the two phases, the meta-stable phase θ ($CuAl_2$) and the S phase (Al_2CuMg), contribute to the strengthening and hardening effects. Thus, improvement of mechanical properties is expected under T6 heat treatment condition. The application of T5 condition is also very promising for finishing parts because it is energy saving and can reduce the costs from heat treatment procedures as compared with that of T6. Therefore, studies on the fatigue property of semisolid A357 alloys under different heat treatment conditions will help us to decide which type of heat treatment is more appropriate for specific services using parts made of semi-solid A357.

In the following sections, research results about the effect of heat treatment on fatigue properties of semisolid A357 aluminum alloys will be presented. S–N data for specimens without heat treatment and heat-treated under two conditions, T5 and T6, will be given. Two-parameter Weibull distribution of fatigue life data for specimens under the two heat treatment conditions will be established. Fracture surface morphology of typical specimens will be given to show the difference in fatigue damage mechanisms associated with different heat treatment conditions.

Experimental methods

Semisolid processing and specimen preparation

Semisolid A357 alloys in the shape of multi-step plates with varied thickness were provided by Citation Southern Aluminum Casting Co., Bay Minnette, Alabama, USA. The semisolid processing includes several steps. First, induction heating and electro-magnetic stirring were used in preparation of the semisolid A357 melt. After the melt was filled into a metal die, intermediate cooling process was used to obtain semisolid mixture with controlled fraction of solid. Following this procedure, compression of the semisolid slurry was conducted. The applied average ram speed in the compression procedure is 60 mm/s for the multi-step plates. The pressure at the head of the ram was kept at 130 MPa. The plates were rapidly quenched in water. Specimens in the shape of circular bar for fatigue testing were prepared from different locations of the semisolid A357. The deformation length of the machined specimens, l_0, is 25 mm and the diameter of the deformation section is 6.35 mm, which is equivalent to a cross section area of 31.67 mm^2.

Heat treatment of the semisolid A357 specimens

The specimens of the semisolid A357 alloy were heat treated under two conditions; without solution treatment: T5 (aged at 170 °C for 4 h) and with solution treatment: T6 (solution treatment at 540 °C for 8 h followed by aging at 170 °C for 4 h).

Fatigue tests and fracture surface examination

Fatigue tests were performed at room temperature of 22 °C under force-controlled conditions at a frequency of 10 Hz using a material testing system (MTS 810). Sinusoidal stress form was used with varied maximum tension peak stress (S) from 105 MPa to 245 MPa. The minimum to maximum stress ratio, R, was kept at 0 so that the cycling was control in the pure tensile state without stress reversal. The fatigue fracture surface of typical specimens under different heat treatment conditions was examined using a Hitachi scanning electron microscope (SEM).

Results and discussion

S–N data

The semisolid specimens in the as-cast state were tested first to provide a baseline of fatigue life under tension/tension cyclic loading conditions with varied maximum loading stress. In this study, the number of cycle, 10^7, is taken as the infinite fatigue life. Thus, the highest applied stress under which a specimen can withstand 10^7 cycles is defined as the fatigue strength of the alloy. The relationship between the maximum stress level, S, and the fatigue life in the form of the number of fatigue cycles, N, is given in Fig. 1. It is found that the specimens without heat treatment have the fatigue strength of 105 MPa as shown in the dotted line for as-cast state in Fig. 1.

Comparison on the fatigue properties of specimens with and without heat treatment was made. The specimens under the two heat treatment conditions T5 and T6 were tested at different stress levels: 245 MPa, 210 MPa, 175 MPa, 140 MPa, and 105 MPa, respectively. The frequency was kept at 10 Hz and the minimum to maximum stress ratio (R) was held at 0. The effect of different heat treatment conditions on the fatigue properties was examined.

The fatigue data for specimens under T5 and T6 heat treatment conditions are also shown in Fig. 1. In the initiation behavior controlled region, i.e. the lower right part of the S~N data profile shown in Fig. 1, no specimen has failed around 10^7 cycles under the cycling condition with the maximum tensile stress of 105 MPa. This indicates that the fatigue strength of the semi-solid A357-T5 and A357-T6 is higher than that of the as processed semisolid A357, 105 MPa. The estimated asymptotic value of maximum stress under which the specimen has infinite fatigue life ($N > 10^7$ cycles in this case), for specimens under the T6 heat treatment condition is about 150 MPa, while this value for specimens under the T5 the treatment condition is about 125 MPa. Thus, the fatigue strength of the semisolid A357-T6 is about 20% higher than that of the semisolid A357-T5. In the propagation behavior controlled region as shown in the upper left section of the S~N plot in Fig. 1, the A357-T6 specimens shown higher stress value than the A357-T5 at the some fatigue cycles. In another word, the A357-T6 has much longer fatigue life than the A357-T5 has at the same applied maximum stress level. Such results provide the information that semisolid A357-T6 parts should have better durability than those under T5 heat treatment condition.

In order to compare the fatigue behavior of the semisolid A357 aluminum alloys with that of conventionally formed aluminum alloys, the S–N data and/or fatigue strength for several casting and wrought aluminum alloys were combined with the S–N data of the semisolid A357 alloys under the two heat treatment conditions of T5 and T6. The results are given in Fig. 2. The conventional casting A357 alloy under T6 heat treatment condition has the lowest fatigue strength of about 70 MPa [18]. Metal die cast A356/357 alloys undergone hot isostatic pressing (HIP) at 100 MPa, 520 °C for 2 h followed by T6 heat treatment [14, 17] showed strength of 90 MPa. It is about 85% of that of

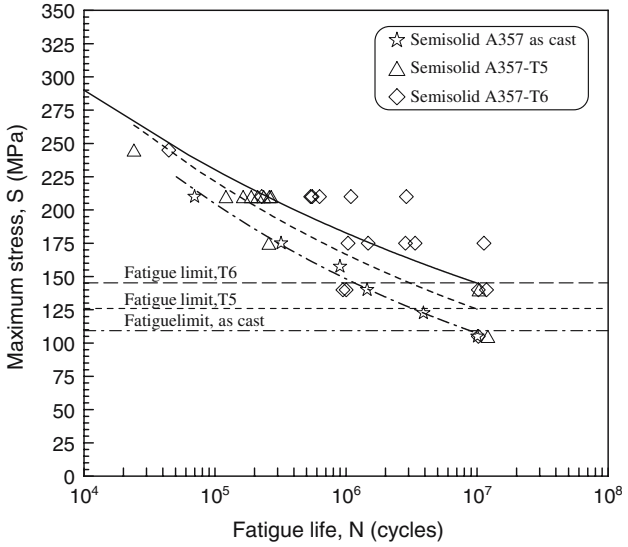

Fig. 1 The relationship between the maximum stress level, S, and the fatigue life in the number of fatigue cycles, N, for semisolid A357

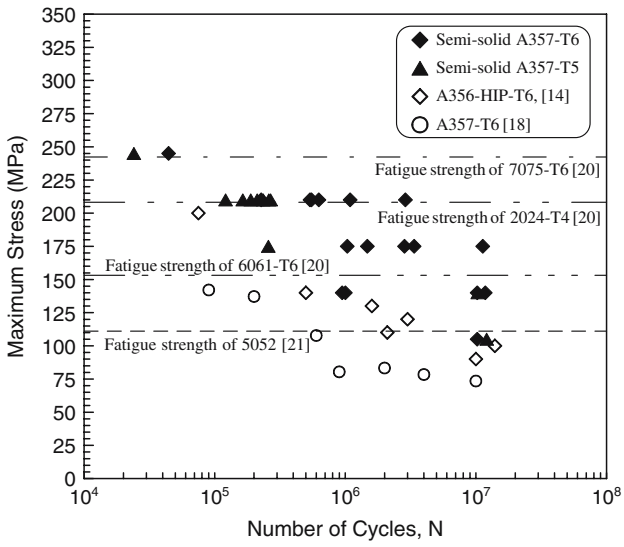

Fig. 2 The comparison of S–N data and fatigue strength of the semisolid A357 alloys under the two heat treatment conditions of T5 and T6 with several casting and wrought aluminum alloys

the semisolid A357 in as cast state, 65% of that of the semisolid A357-T5, and it is much lower than that of the semi-solid A357-T6. Although most of the high strength forged aluminum alloys such as 2024-T4 and 7075-T6 displayed higher fatigue strength [20] than that of the semisolid A357-T6 and A357-T5, as can be seen from the results in the form of dotted lines in Fig. 2. The fatigue strength of semisolid A357-T5 and A357-T6 alloys is still higher than that of the 5052-T6; 110 MPa [22], and comparable to that of the 6061 under T6 heat treatment condition. Thus, semisolid aluminum alloy parts can compete with some of the wrought alloys. In some cases, it is possible to replace the wrought alloy parts with semisolid components for reducing costs.

Comparison of the fatigue data obtained at stress ratio of $R = 0$ for A357-T6 in this work with those obtained at $R = -1$ in [21] was made. As shown in Figure 8 of [21], at $R = -1$, a 10^5 cycle fatigue life corresponds to the fatigue strength of 170 MPa and a 10^4 cycle fatigue life corresponds to the fatigue strength of 220 MPa. In this work, a 10^5 cycle fatigue life corresponds to the fatigue strength of 125 MPa and a 10^4 cycle fatigue life corresponds to the fatigue strength of 290 MPa, as shown in Fig. 1. This indicates that the fatigue property of the semisolid A357-T6 is sensitive to stress reversal. Tension stress followed by compressive stress reversal accelerates fatigue damage of the material.

Fatigue life distribution

Weibull statistics [23] has been widely used to describe the failure behavior of materials under tension, compression or even mixed stress mode conditions [24]. A two-parameter Weibull distribution graph of fatigue life for the semisolid A357 heat-treated under T6 and T5 conditions was constructed to show the statistical significance of heat treatment. Fatigue tests were performed under the same cyclic loading conditions with the maximum stress level of 210 MPa, and the stress ratio of 0. The fatigue failure probability of the two types of specimens as a function of fatigue life in a natural logarithm Weibull plot; $\ln\{\ln[1/(1-F)]\}$~N was obtained. F is the probability of failure. N is the fatigue life. The fatigue life, for each heat treatment condition was evaluated on at least seven specimens of identical geometry. The commonly used ordering/ranking statistics together with a linear regression as used by Wang et al. [14, 17] is adopted here to evaluate the characteristic fatigue life, N_0, and the Weibull modulus, m, for both heat treatment conditions.

The Weibull distribution plot of Fig. 3 reveals a linear behavior of fatigue data for specimens under

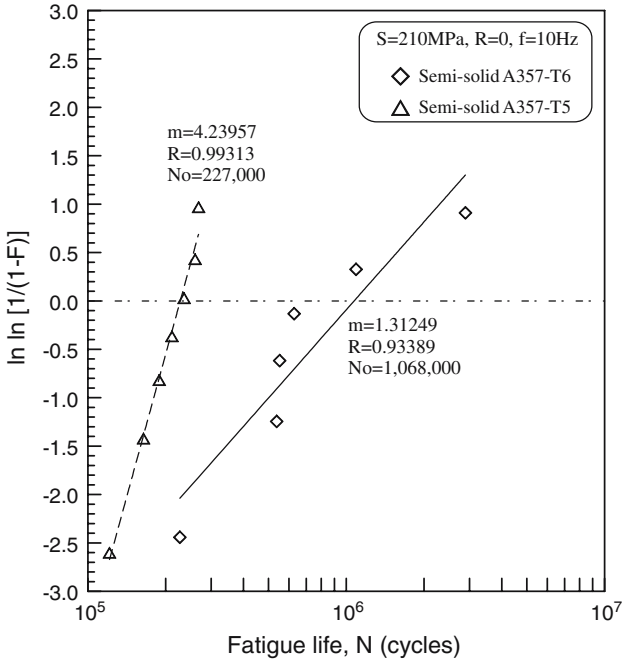

Fig. 3 Two-parameter Weibull distribution plots for the semisolid alloy showing statistical significance in fatigue life due to different heat treatment

both heat treatment conditions. This indicates that the Weibull distribution can describe the fatigue behavior of the semisolid A357 alloys. The effect of different heat treatment conditions on the fatigue properties of the alloys is also shown. The specimens under the T5 heat treatment condition showed a much lower characteristic life than that of the specimens heat treated under T6 condition. The characteristic fatigue life of the semisolid A357-T5 is about 227,000 cycles, while this value for the semisolid A357-T6 is over 1,068,000 cycles. Also found here is the difference in the Weibull modulus of the semisolid A357-T6 and the semisolid A357-T5. The T5 specimens displayed much better linearity than the T6 specimens. The Weibull modulus, m, for the T5 specimens is 4.23957, while this value for the T6 specimens is only 1.31249. This is the explanation of the more pronounced data scattering tendency for the T6 specimens. Such a result is in agreement with that the T6 specimens showed higher notch sensitivity so that most of the fatigue specimens broke near the radius region of the deformation section where stress concentration is higher than other places.

Fatigue damage evolution in view of cumulative strain

The long time cyclic deformation behavior of specimens under different heat treatment conditions was studied. The accumulated strains for different number

of fatigue cycles were captured by a level crossing data acquisition mode. That is, an arbitrary stress level was given, and strain at this level was intermittently recorded at different number of cycles until the specimen broke. In this study, we set the stress level at 25 MPa. The interval of recording strain data is 1,000 cycles. The results of accumulated strains are shown in Figs. 4a and b for T5 and T6 heat-treated specimens, respectively. The specimens under T5 and T6 heat treatment conditions show different behavior of fatigue damage accumulation. In the initial stage, a fatigue threshold of strain hardening around the crack tip is shown for both specimens, but the extent of drop in strain is very different. The amount of decreased strain for the T6 specimen is less than one fifth of that of the T5 specimen. Thus, the T6 specimen has better fatigue endurance than the T5 specimen if crack initiation dominates the fatigue life.

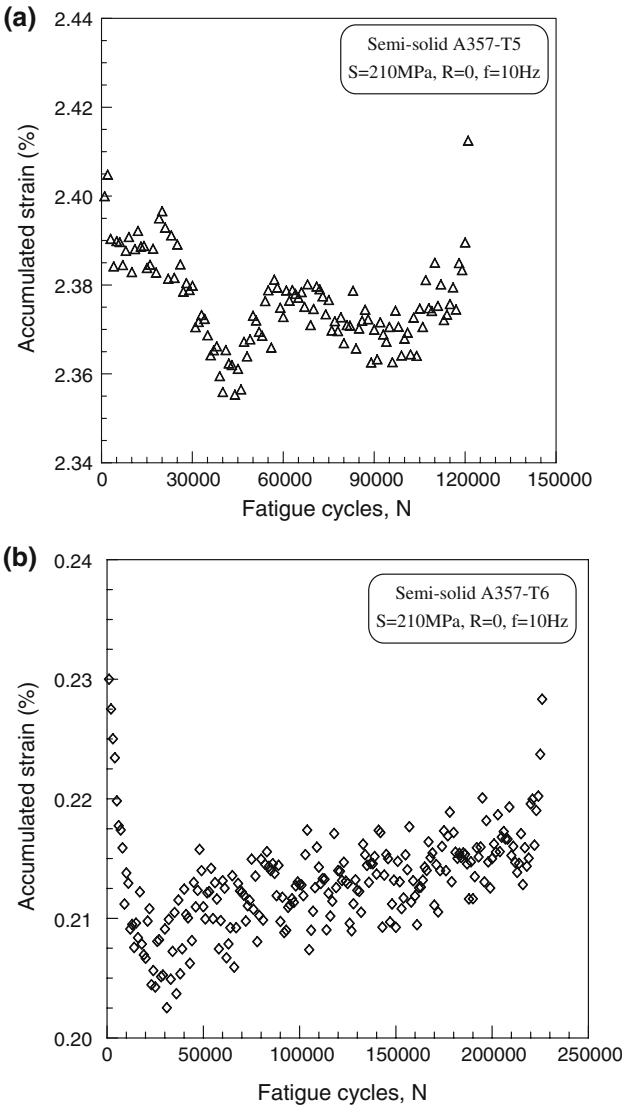

Fig. 4 The relationship between accumulated strains and fatigue cycles. (**a**) T5 heat treatment (**b**) T6 heat treatment

In the fatigue propagation domain; i.e. the middle section of Figs. 4a and b, the T5 specimen displayed multistage softening and hardening behavior. The data of cumulative strain are distributed in a zig-zag zone. Nevertheless, the T6 specimen just showed very limited softening behavior as evidenced by the slight increase in accumulated strain in the stable crack growth stage of the middle section of Fig. 4b. This reveals that the T5 specimen has lower granular strength than that of the T6 specimen. It is also shown in Fig. 4a and b that the fatigue stable crack growth region of the T6 specimen is much bigger than that of the T5 specimen, indicating a lower sub-critical crack growth speed for the T6 specimen. Generally, longer stable crack growth life means that defective parts have longer service lifetime. Thus, the fatigue damage tolerance of the T6 specimen should be higher. The last data point, at a much higher level of strain than previous points, in both Fig. 4a and 4b stands for the unstable crack growth in the two specimens.

Fracture surface and fatigue fracture mechanisms

Fatigue fracture surface morphology examination using scanning electron microscope (SEM) was performed on the specimens of the semisolid A357 alloy being heat treated under two different conditions, T5 and T6, to identify their fatigue damage and fracture mechanisms. The specimens were fatigue tested at the stress level of 210 MPa with the same stress ratio of $R = 0$. The global view of the fatigue fracture surface for two typical specimens under each heat treatment condition is very similar, which can be schematically shown in Fig. 5. The initiation site is located at the edge of the circular bar-shaped specimens. The fatigue crack growth is in a fan shape way; irradiating from the initiation site to the deep section of the specimens. Region I, the crack initiation region on the fracture surface of the specimens is very small, only about 0.3 mm^2 as determined by quantitative microscopic analysis through the area measurement of a series of low magnification fractographs. The rest of the fracture surface can be divided into two distinct regions according to the morphological features. Region II stands for the stable crack propagation, covering 8 mm^2 of the fracture surface and the area is pretty bright under natural lighting. The third region is denoted as Region III. This is the crack unstable propagation region with the features of fast crack growth. The appearance of this region is of dark grey color. The third region takes about 21 mm^2.

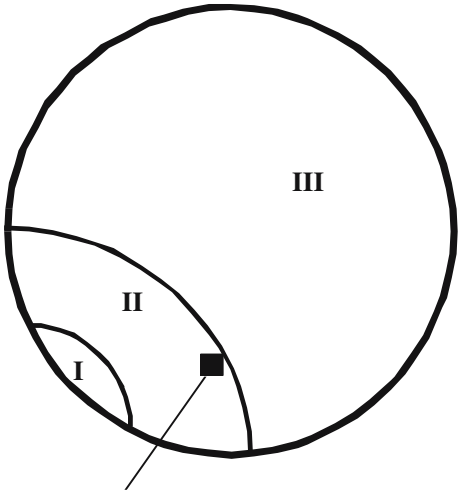

Fig. 5 Schematic drawing of the global view of the fatigue failed semisolid A357 specimens under T5 and T6 heat treatment conditions

The morphological features of fracture surface in the stable crack growth region are especially interesting because they carry the message related to the micro-plasticity of the materials at the growing crack tip. Analysis of the features in this region would allow us to have a more comprehensive understanding of the failure mechanisms of semisolid formed parts under different heat treatment conditions. Figure 6a, an SEM micrograph taken from the fracture surface of the T5 specimen, shows the fracture surface features in the ending zone of the second region (Region II in Fig. 5). Pulled-up gains indicate a considerable plastic deformation associated with the stable crack growth. Fine dimple carrying texture generated by the cyclic strain softening process was found. Traces of void coalescence can be seen along grain boundaries. These features indicate a ductile fracture mechanism related to the stable crack growth. The multistage, alternative strain softening and hardening in this region, as demonstrated in Fig. 6a, is well recorded. This is featured by the separation of grains at different levels and the formation of the fracture ridges, as shown in the middle part of Fig. 6a. The upper right part of the micrograph displays cleavage tongue like facets, indicating the accelerated crack growth speed at the end of the second region.

The second region of fatigue failed T6 is shown in Fig. 6b, an SEM image taken from the same location of Region II as illustrated in Fig. 5. Obviously, the second region of the fractured specimen under T6 heat treatment condition displayed a much less plastic deformation than that of the specimen under T5 heat treatment condition. For the T6 specimen, transgranular

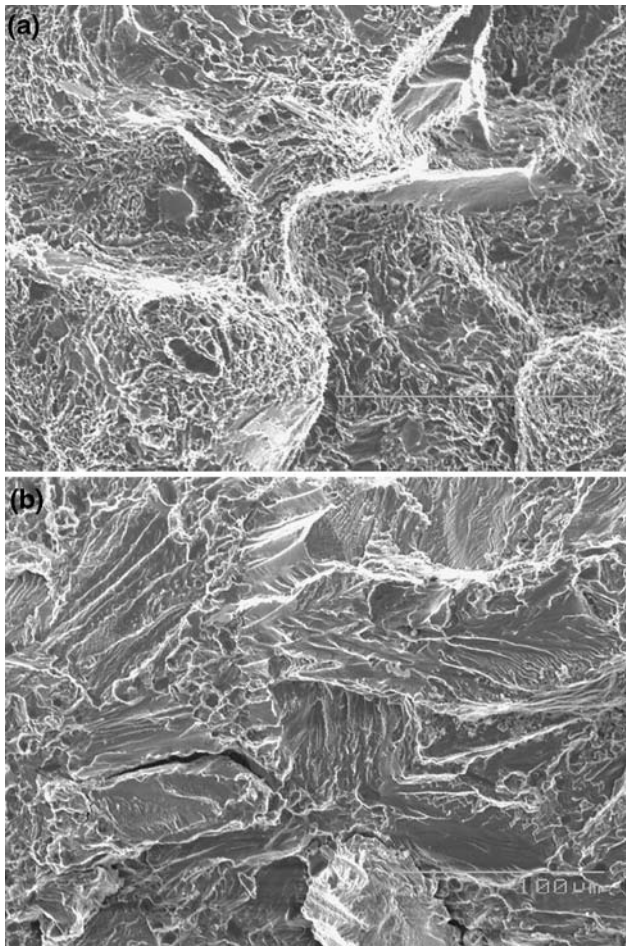

Fig. 6 SEM micrographs taken from the crack stable growth region showing fatigue damage features of the specimens: (**a**) under T5 heat treatment condition, (**b**) under T6 heat treatment condition. The length of scale marker is 100μm

fracture features are well pronounced. In the upper section of this micrograph, ductile tearing ridgelines and cleavage tongues can be seen. The existence of transgranular tearing zones is another feature in the stable crack growth region. These tearing zones are characterized by pulled up ridgelines aligned in irradiated patterns which are similar to ductile cleavage herring bones or river patterns in other types of ductile metallic alloys, for example, an A508 class 3 steel [25]. Such morphological features reveal a very high resistance associated with the stable crack growth. These fractographic features can also explain the gradual increase in the accumulated strains of the fatigue specimen as shown in Fig. 4b. Although intergranular voids and cracks can be found in the lower part of the micrograph in Fig. 6b, such intergranular discontinuities are not the dominant features accompanying the crack propagation. Still the transgranular separation controlled the stable crack growth. This

indirectly reflects that the semisolid T6 has both considerably higher grain strength and intergranular strength than those of the T5 specimen, which is the result of the homogenous precipitation and hardening following the solution treatment in the T6 heat treatment schedule.

Conclusions

(1) The fatigue properties of the semisolid A357 are sensitive to heat treatment conditions. Without heat treatment, the as cast specimens showed the lowest fatigue strength. The specimens heat treated under T6 condition displayed higher fatigue strength than those under T5 heat treatment condition.
(2) As compared with conventionally cast alloys, the semisolid A357 under both heat treatment conditions has much higher fatigue strength. The fatigue strength of the semisolid A357 is also higher than that of metal die cast A357 condensed by HIP (hot isostatic pressed under 100 MPa at 520 °C for 2 h). Fatigue property of several wrought aluminum alloys was compared with that of the semisolid A357. It is found that the fatigue strength of the semisolid A357 is comparable to that of the 5052-T6 and 6061-T6, but lower than that of the 2024-T4 and 7075-T6.
(3) Weibull distribution is applicable for describing the fatigue property of the semisolid A357. The two-parameter Weibull distribution plots of fatigue data for specimens under the two heat treatment conditions show the statistical significance of the effect of heat treatment conditions on fatigue crack propagation life. The characteristic fatigue life of the semisolid A357-T6, 1,068,000 cycles, is as four times high as that of the semisolid A357-T5, 227,000 cycles, at the same maximum stress level of σ_{max} = 210 MPa.
(4) In the stable crack propagation region, the A357-T5 showed fatigue damage species of fine dimples, severely deformed grains, void coalescence and pronounced fatigue fracture ridges, while the A357-T6 displayed much less plastic deformation as revealed by the fatigue damage features of intergranular cracks, tearing and transgranular ductile cleavage patterns.

Acknowledgements This work is supported in part by NASA through Auburn University Materials Processing Center. The semisolid casting materials were provided by Citation Southern Aluminum Castings Co., Bay Minette, Alabama, USA. YXG acknowledges the assistance from Mr. Amit Suryawanshi in machining the fatigue test specimens. We appreciate the reviewer(s) for the valuable suggestions for modifying the paper.

References

1. Spencer DP, Mehrabian R, Flemings MC (1972) Metal Trans 3:1925
2. Kirkwood DH (1993) Int Mat Rew 39:173
3. Jung HK, Seo PK, Kang CG (2001) J Mater Process Technol 113:568
4. Kang CG, Jung KD (2001) J Mater Eng Perform 10:419
5. McLelland ARA, Hendeeson NG, Atkinson HV, Kirkwood DH (1997) Mater Sci Eng A232:110
6. Kapranos P, Ward PJ, Atkinson HV, Kirkwood DH (2000) Mater Des 21:387
7. Witulskil T, Morjan U, Niedick I, Hirt G (1998) The thixoformability of aluminum alloys. In: Bhasin A, Moore JJ, Young KP, Midson S (eds) Proceedings of the fifth international conference on semisolid processing of alloys and composites, Golden (CO), p 353
8. Kapranios P, Liu TY, Atkinson HV, Kirkwood DH (2001) J Mater Process Technol 111:31
9. Jung HK, Kang CG (2002) J Mater Process Technol 120:355
10. Kang CG, Son YI, Youn SW (2001) J Mater Process Technol 113:251
11. Barkhudarov MR, Bosnisz CL, Hirt CW (1996) Three-dimensional thirotropic flow model. In: Kirkwood DH, Kapranos P (eds) Proceedings of the fourth international conference on semisolid processing of alloys and composites, Golden (CO), p 110
12. Kapranos P, Barkhudarov MR, Kirkwood DH (1998) Modeling of microstrauctural breakdown during rapid compression of semi-solid alloy slurries. In: Bhasin A, Moore JJ, Young KP, Midson S (eds) Proceedings of the fifth international conference on semisolid processing of alloys and composites, Golden (CO), p11
13. Avelle M, Belingardi G, Cavatorta MP, Doglione R (2002) Int J Fatigue 24:1
14. Wang QG, Apelian D, Lados DA (2001) J Light Metals 1:73
15. Buffiere JY, Savelli S, Jouneau PH, Maire E, Fougeres R (2001) Mater Sci Eng A361:115
16. Tan YH, Lee SL, Wu HY (1996) Int J Fatigue 18:137
17. Wang QG, Apelian D, Lados DA (2001) J Light Metals 1:85
18. Reinhart TL (1996) Fatigue and fracture properties of aluminum alloy castings. In: Lampman S (ed) Fracture and fatigue, vol 19. ASM Metals Handbook, Materials Park (OH) ASM International, p 813
19. Beck T, Lang KH, Lohe D (2001) Mater Sci Eng A319–321:662
20. Buck A (1988) Fatigue data sheets. Fatigue strength calculation, Materials science surveys No.6, Brookfield, Trans Tech Publications, p 383
21. Bergsma SC, Li X, Kassner ME (2001) Materials Sci Eng A297:69
22. Wang MZ, Kassner ME (2002) J Mater Eng Perform 11:167
23. Weibull W (1951) J Appl Mechanics 18:293
24. Williams PT, Bass BR, McAfee MJ (2000) Application of the Weibull methodology to a shallow-flaw cruciform bend specimen tested under biaxial loading conditions. In: Halford GR, Gallagher JP (eds) Fatigue and fracture mechanics, ASTM STP 1389, vol.31. West Conshohocken (PA), American Society for Testing and Materials, p 242
25. Anderson TL (1991) In: Fracture Mechanics Fundamentals and Applications CRC Press, Boca Raton, p 714